RSC Advances

ROYAL SOCIETY OF CHEMISTRY

www.rsc.org/advances

RSC Advances

RSCPublishing

PAPER

Sequential Solvent Casting for Improving the Structural Ordering and Electrical Characteristics of Polythiophene Thin Films†

Cite this: RSC Adv., 2014

Received ooth XX 2014,
Accepted ooth XX 2014

DOI: 10.1039/xoxxooooox

www.rsc.org/

Shinae Kim[a], Boseok Kang[b], Minjung Lee[c], Seung Goo Lee[d], Kilwon Cho[b], Hoichang Yang[c,*], Yeong Don Park[a,*]

We developed a facile post-deposition method for preparing high-performance organic transistors using direct solvent exposure. The morphological, optical, and electrical properties of poly(3-hexylthiophene) (P3HT) films were profoundly influenced by the solubility of P3HT in a solvent. Exposure to an optimized binary solvent mixture comprising methylene chloride and toluene efficiently improved the morphology and molecular ordering in a conjugated polymer thin film. The improved ordering was correlated with improved charge carrier transport in the field-effect transistors (FETs) prepared from the films. The correlation between the thin films' structural features and the electrical properties of the films guided the identification of an appropriate binary solvent mixing ratio and characterized the influence of the physical properties on the electronic properties of solvent-exposed P3HT films in an FET.

1. Introduction

Recent years have seen significant improvements in the performances of organic field-effect transistors (FETs) based on π-delocalized conjugated polymers.[1-6] The primary performance requirement for semiconducting polymer thin films prepared from solution processing techniques, such as spin-coating,[7] bar coating,[8] ink-jet printing,[9] and screen printing, is the attainment of a high charge carrier mobility.[10] To this end, both the design of polymer structures and the effects of the interchain polymer–polymer interactions on the interpolymer ordering structure may be optimized. The interchain interactions are mediated predominantly through weak van der Waals interactions that can introduce structural defects in a polymer layer during film formation. Structural defects arising from poorly organized arrangements can result in poor electrical characteristics by limiting intrachain charge carrier transport. Intrachain charge carrier transport occurs via charge carrier hopping between disordered segments through weak intermolecular π-π coupling interactions. For this reason, the self-assembled structures of π-conjugated polymers are important for determining a film's optical and electrical properties.

Toward the aim of enhancing the organic FET device performance, several processing parameters have been extensively investigated, including choice of solvent,[11,12] film formation method[13-15] and post-treatments such as thermal[16] or solvent annealing steps.[17,18] Many groups demonstrated solution crystallization by using non-solvents or additive to induce polymer nanocrystal in the solution states. However care must be taken so that the volume ratio of added solvent, aging time, and polymer concentration is not sufficiently high so that aggregate size increases to the point of incipient precipitation, which leads to heterogeneous films with coarse features. Typical solution crystallization is complicated process and extremely limited in the choice of solvent. Therefore post-treatment steps are nearly always required for improving the molecular order and charge carrier mobility in a film.[19] Thermal annealing steps are not compatible with flexible substrates that have a low glass transition temperature because the steps can degrade the gate dielectric layer. Solvent vapor annealing is not suitable for large-scale continuous film processes. The chain mobility of a polymeric backbone can be improved in the presence of a solvent with a high vapor pressure; however, such solvents can dissolve or de-wet the cast films. These post-treatment processes such as thermal and solvent-vapor annealing require relatively long durations of at least 20 minutes.

Direct contact between a solvent and a moderately soluble deposited polymer film can potentially be used to control the morphology and structural ordering in a polymer thin film.[20-22] Direct contact with a solvent can mobilize the polymer chains to facilitate reorganization over short periods of time. Solvent-assisted chain reorganization processes require the careful selection of the solvent so as to avoid severely damaging the film. In general, the solubility of a polymer in a solvent is primarily governed by the various interactions between the polymer chains and the solvent molecules.[23] The dissolving power of a solvent can be simply controlled using a binary solvent system comprising two solvents with different dissolving powers in aromatic and aliphatic solvents. Post-treatment approaches involving a binary solvent can be

effectively applied to fabricate high-performance polymer FETs.

In this report, we present a systematic study of a simple post-deposition method for controlling the structural and electrical characteristics of spin-coated polythiophene thin films through direct exposure to binary solvents. Simply spin-casting a mixed solvent composed of a marginal solvent and a small amount of a good solvent onto a polymer thin film dramatically improves the intermolecular ordering in the films, the charge carrier mobilities, and the polymer FET device performance. The structural and electrical characteristics of as-spun polythiophene thin films or thin films exposed to poor or marginal solvents were investigated and compared.

2. Experimental details

2.1 Preparation of Polythiophene Thin Films and FET Devices

Poly(3-hexylthiophene) (P3HT) obtained from Rieke Metals, Inc. (regioregularity ~91%, molecular weight, M_w = 20–30 kDa) was used as received without further purification. Highly doped Si was used as a gate electrode substrate. A thermally grown 300 nm thick SiO_2 layer was employed as a gate dielectric (capacitance = 10.8 nF cm^{-2}). Hexamethyldisilazane (HMDS) (Aldrich) was used as an organic interlayer material between the organic active material and the dielectric layer and was applied to the SiO_2 substrate via spin-casting. A solution of P3HT (10 mg/mL) in anhydrous chlorobenzene (Aldrich) was spin-coated onto the substrate (1500 rpm, 60 s). A variety of solvents, including ethanol, acetone (ACT), methylene chloride (MC), toluene (TOL), and binary mixtures composed of MC and TOL (volume ratios of 3:1, 2:1, and 1:1) were spin-coated onto the as-spun P3HT films (1500 rpm, 60 s). P3HT-based FETs were formed by evaporating gold through a shadow mask (channel length = 100 μm and channel width =1500 μm). Identical P3HT films were fabricated on transparent glass substrates instead of Si substrates in preparation for the UV-Vis absorption measurements.

2.2 Characterization

UV-Vis absorption spectra were acquired using a UV-Vis spectrophotometer (CARY-5000, Varian). The thickness values of the cast P3HT films were measured using an ellipsometer (J. A. Woollam Co. Inc.). The film morphologies were characterized by atomic force microscopy (AFM, Multimode IIIa, Digital Instruments). Two-dimensional grazing incidence X-ray diffraction (2D GIXD) studies were performed at the 3C and 9A beamlines of the Pohang Accelerator Laboratory, Korea. The electrical performances of the organic FETs were characterized using a semiconductor analyzer (Keithley 4200) at room temperature (RT). The field-effect mobility (μ_{FET}) and threshold voltage (V_T) were estimated in the saturation regime (V_D = –80 V) according to the equation:[24]

$$I_D = \frac{W}{2L}\mu_{FET}C_g\left(V_G - V_T\right)^2$$

where I_D is the drain current, C_g is the capacitance of the gate dielectric, and V_G is the gate–source voltage.

3. Results and discussion

The effects of direct contact with various solvents, including ACT, MC, TOL, and binary solvent mixtures of MC and TOL (volume ratios of 3:1, 2:1, and 1:1) on the crystalline structures and electrical properties of the P3HT thin films were investigated. Figure 1a shows the UV-Vis absorption spectra of the spun-cast P3HT thin films before or after exposure to the above solvents. The spectrum of the as-spun P3HT thin film revealed a dominant peak at λ = 534 nm, corresponding to the intrachain π-π* transition of P3HT, and a minor shoulder at lower energies (λ ~ 605 nm).[25-28] After exposing the P3HT thin films to the solvents, the UV-Vis absorbance intensities were found to decrease 3–16%, depending on the dissolving power of the solvents, as a result of film thinning (determined by ellipsometry analysis, see Figure S1). ACT and TOL are, respectively, poor and good solvents for P3HT at RT, whereas MC is a marginal solvent and solubilizes only the relatively low M_W moieties of P3HT.

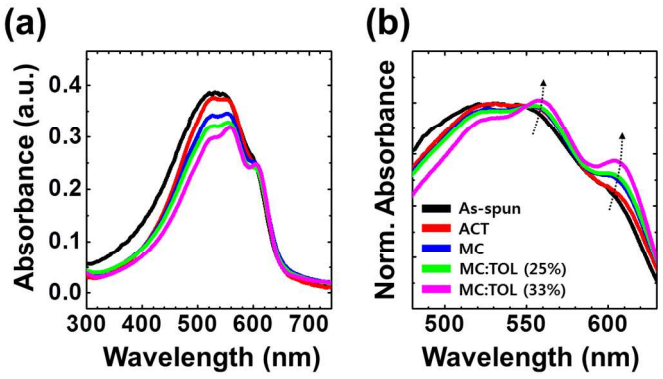

Figure 1. (a) UV-Vis absorption spectra of the P3HT thin films before and after exposure to various solvents, and (b) magnified normalized UV-Vis absorption bands. The solubility of P3HT in each solvent increases along the direction of the arrow.

The ACT-exposed P3HT films showed no changes in either the UV-Vis absorbance or the film thickness. After exposure to MC or the MC/TOL binary mixtures, the peak intensities of the absorbance spectra decreased dramatically as the TOL fraction increased. TOL is a good solvent for both the aromatic backbones and the alkyl side chains of P3HT. In this case, the thickness values of the P3HT films decreased monotonically from 44.5 nm, (for the as-spun films) to 40.4 nm (for the MC/TOL 33% exposed films, see Figure S1). This result agreed well with the decrease in the UV-Vis absorbance peak intensity.

The characteristics of the P3HT absorption band varied considerably after exposure to the binary solvents, as shown in Figure 1b. The addition of TOL to the binary solvents resulted in the introduction of additional absorption bands at lower energies (λ = 558 nm and 605 nm). These features were attributed to the dramatic increase in the number of ordered P3HT aggregates containing interchain π-π stacking interactions, i.e., the effective π-conjugation length increased;[29] however, direct exposure to a high TOL content solvent, i.e., MC/TOL50% or the TOL systems, caused serious film damage. These solvent mixtures were excluded from the remainder of the experiments.

Figure 2 shows the AFM morphologies of the P3HT films. AFM phase images of the as-spun films revealed nano-

aggregates 20 nm in size that formed a percolating network with a smooth surface characterized by a root mean square surface roughness (R_q) of 0.89 nm (Figure 2a). The ACT-exposed films produced a similar morphology and roughness because ACT is a poor solvent for P3HT (Figure 2b). After exposure to MC or its major mixtures with TOL, the P3HT films tended to display nanofibrillar network structures that increased R_q, but maintained a homogeneous dielectric surface coverage (Figures 2c-2f). The morphological results revealed that the binary solvent exposure method could effectively induce intermolecular π-π stacking among semiconducting polymers in a predeposited film. Previous studies of alcohol-exposed P3HT films have not reported the observation of this type of morphological change after exposure to MC or a binary solvent system because alcohol is a poor solvent of P3HT and provides an insufficient driving force for the reorganization of the long polymer chains.[30] The entropy and polymer–solvent attractions in polymer–solvent systems determine the solubility of the polymer in a solvent. In a poor solvent, the polymer chains tend to be tightly balled up.[31] Therefore, the observation of larger P3HT aggregates in the films exposed to binary solvent was attributed to two effects: enhanced mobility as a result of exposure to the good solvent, and enhanced segregation among the π-conjugated P3HT molecules as a result of exposure to the marginal solvent. MC, a marginal solvent, poorly solvated P3HT at RT.[32]

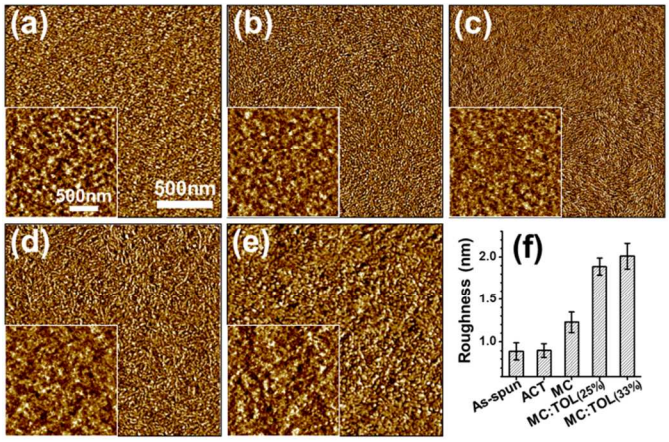

Figure 2. AFM phase images of P3HT films exposed to the various solvents: (a) as-spun, homo solvents, such as (b) acetone (ACT) and (b) methylene chloride (MC), and binary solvents comprising MC and toluene (TOL) in mixing ratios of (d) 3:1 and (e) 2:1, respectively. The inset shows the height images of each film. (f) The root mean square roughness of the film surface is provided.

The impact of direct solvent exposure on the electrical properties (the *I-V* characteristics) of a FET prepared from a P3HT film were systematically characterized (see Figure 3a and Figure S2). The variations in the average field-effect mobility (μ_{FET}) and on/off current ratio (I_{on}/I_{off}) are summarized in Figure 3b. The best value of μ_{FET} was obtained in the P3HT film exposed to MC:TOL(33%), 3.5×10^{-3} cm^2 V^{-1} s^{-1}. This μ_{FET} was a factor of 6 greater than the value (5.1×10^{-4} cm^2 V^{-1} s^{-1}) obtained from the FETs prepared using an as-spun P3HT film. The MC:TOL(33%)-exposed P3HT film displayed a significantly better I_{on}/I_{off} ratio and subthreshold swing (*SS*) compared to the as-spun film. Charge transport in an FET occurs in the vicinity of the semiconductor–gate dielectric interface; therefore, this result suggested that the prevalence of interfacial charge traps in the binary-solvent exposed P3HT film had decreased and that binary solvent exposure can alter both the topmost film structure and the buried region near the HMDS-treated SiO_2 dielectric surface. The structural variations near the gate dielectric were mainly attributed to the rapid diffusion of TOL molecules into the loosely packed π-conjugated polymer chains of the as-spun P3HT films.

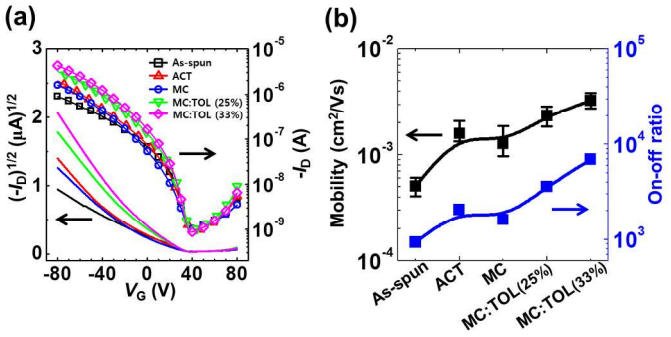

Figure 3. (a) Transfer characteristics (I_D–V_G) of FETs (V_D = –80 V) fabricated from P3HT thin films exposed to a variety of solvents. (b) Summary of the device characteristics obtained from the P3HT FETs.

The crystal structures of the P3HT films before or after direct solvent exposure were characterized using 2D GIXD methods. Figure 4 shows the 2D GIXD patterns obtained from the P3HT films before or after exposure to various solvents. As-spun P3HT displayed X-ray reflections of the (*010*) crystal planes along both the Q_z (out-of-plane) and Q_{xy} (in-plane) axes, indicating that a large fraction of the P3HT molecules assumed a face-on chain conformation with respect to the HMDS-SiO_2 dielectric surface. By contrast, the P3HT films that had been directly exposed to a solvent consistently displayed strong X-ray reflections from the (*h00*) and (*010*) crystal planes along the Q_z and Q_{xy} axes, respectively. This result suggested that most of the P3HT molecules assumed an edge-on chain conformation with standing side chains on the dielectric, as illustrated in Figure 4.[33] The degree of crystallinity and chain orientations in these films depended on the solvent type, as demonstrated based on the 1D out-of-plane and in-plane X-ray profiles extracted from the 2D GIXD patterns (see Figure 5).

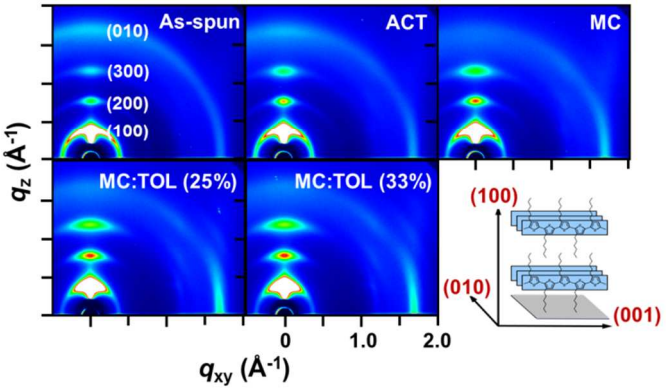

Figure 4. 2D GIXD patterns of the P3HT thin films: as-spun or exposed to a variety of solvents. The schematic illustration provides information about the P3HT crystal structure, with plane indices.

Along the Q_z (out-of-plane) axis, the X-ray profile of the as-spun P3HT film showed relatively weak (h00) reflections and strong (010) reflections, which corresponded to intermolecular backbone layer and π-π stacking plane distances of 16.7 Å and 3.8 Å, respectively (Figures 5a and 5b).[34] Direct solvent exposure to the binary solvents significantly increased the peak intensities of the (100) reflection in the out-of-plane profiles, whereas the (010) reflections immediately decreased (Figures 5a–5b). Although the films were relatively thin (Figure S1), the intensities of the out-of-plane (100) Bragg peak gradually increased with the dissolving power of the solvent, indicating that the binary solvents facilitated the formation of widespread structural ordering. The position of the (100) reflection gradually shifted to higher q_z values and the lamella spacing in the (100) plane decreased slightly as the dissolving power of the solvent increased, indicating a much closer packing of the P3HT chains (see Figure S3). In contrast with the trend followed by the intensity of the out-of-plane (010) reflections, the intensities of the in-plane (010) reflections gradually increased with the dissolving power of the cast solvents (Figure 5c, 5d), indicating improved π-π interchain stacking along the in-plane direction.

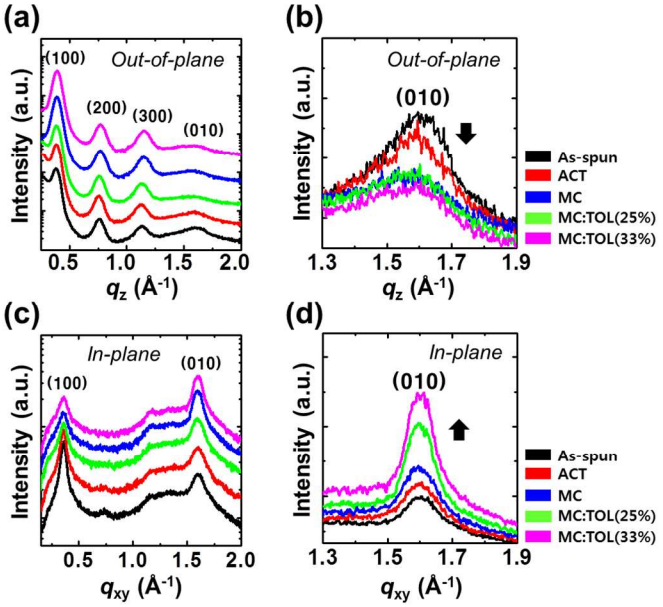

Figure 5. X-ray intensity profiles for the various solvent-exposed P3HT thin films along (a) the out-of-plane, and (c) the in-plane directions. (b) and (d) show magnified profiles of the (010) peaks in each scan direction. The solubility of P3HT in each solvent increases along the direction of the arrow.

Overall, the GIXD measurements suggested that exposure of the as-spun P3HT films to a moderately good solvent improved the crystallinity of the P3HT films. The chain orientations favored charge carrier transport in the organic FETs.[35] The lamella packing density in the P3HT films, therefore, increased.[36] The notable changes introduced during binary solvent exposure may have resulted from the effective penetration of the marginal solvent, assisted by the good solvent, which increased the polymer chain mobility and induced the extent of interchain π-π stacking interactions of the P3HT alkyl side chains. Poly(3-alkylthiophene)s molecules consist of a rigid aromatic backbone and solubilizing alkyl chains at the 3-position of the thiophene. Aliphatic organic solvents predominantly dissolve the alkyl side chains instead of the aromatic backbone, while aromatic organic solvents such as toluene could mostly solvate the aromatic core of polymer chains. Therefore, combination of aliphatic and aromatic solvents would effectively induce the polymer-chain mobilize and reorganize compared to use of homo solvent with suitable solubility.[37] The enhanced field-effect mobility in the modified P3HT FETs was attributed to the improved structural order and preferred chain orientations.

4. Conclusion

In summary, we investigated the effects of directly exposing P3HT films to solvents having various solubilities on the structural ordering and FET device performance. Exposing the P3HT films to a moderate solvent changed the film morphology and produced a thin film with a higher crystallinity and edge-on orientation, as revealed by the UV absorption, AFM, and GIXD measurements. The changes in the molecular ordering and orientation in the P3H thin film translated into a higher charge carrier mobility. The optimization method is simple offers practical advantages for the fabrication of high-performance polymer devices.

Acknowledgements

This research was supported by the Incheon National University Research Grant in 2013 and by Basic Science Research Program through the National Research Foundation of Korea (NRF) funded by the Ministry of Science, ICT & Future Planning (2012R1A1A1004279). The authors thank the Pohang Accelerator Laboratory for providing the synchrotron radiation sources at 3C and 9A beam lines used in this study.

Appendix A. Supplementary material

Supplementary material associated with this article can be found, in the online version, at http://

Notes and references

[a] Department of Energy and Chemical Engineering, Incheon National University, Incheon 406-772, Korea
[b] Department of Chemical Engineering, Pohang University of Science and Technology, Pohang 790-784, Korea
[c] Department of Advanced Fiber Engineering, Optoelectronic Hybrids Research Center, Inha University, Incheon, 402–751, Korea
[d] Department of Chemical Engineering, Massachusetts Institute of Technology, Cambridge, Massachusetts 02139, USA
[⊥]S. K. and B. K. contributed equally to this work.
* Corresponding author. Tel: +82-32-835-8679; Fax:+82-32-835-0797.
E-mail address: hcyang@inha.ac.kr (H.Yang), ydpark@incheon.ac.kr (Y. D. Park)

1 J. Hou, H. Y. Chen, S. Zhang, R. I. Chen, Y. Yang, Y. Wu and G. Li, *J. Am. Chem.*, 2009, **131**, 15586.
2 Y. D. Park, J. A. Lim, H. S. Lee and K. Cho, *Mater. Today*, 2007, **10**, 46.
3 H. Klauk, *Chem. Soc. Rev.*, 2010, **39**, 2643.

4 C. D. Dimitrakopoulos and P. R. L. Malenfant, *Adv. Mater.*, 2002, **14**, 99.
5 T. Someya, H. E. Katz, A. Gelperin, A. J. Lovinger and A. Dodabalapur, *Appl. Phys. Lett.*, 2002, **81**, 3079.
6 J. A. Lim, F. Liu, S. Ferdous, M. Muthukumar and A. L. Briseno, *Mater. Today*, 2010, **13**, 14.
7 D. M. DeLongchamp, B. M. Vogel, Y. Jung, M. C. Gurau, C. A. Richter, O. A. Kirillov, J. Obrzut, D. A. Fischer, S. Sambasivan and L. J. Richter, *Chem. Mater.*, 2005, **17**, 5610.
8 F. C. Krebs, *Org. Electron.*, 2009, **10**, 761.
9 T. Aernouts, T. Aleksandrov, C. Girotto, J. Genoe and J. Poortmans, *Appl. Phys. Lett.*, 2008, **92**, 033306-1.
10 F. C. Krebs, *Sol. Energy Mater. Sol. Cells*, 2009, **93**, 394.
11 J. F. Chang, B. Sun, D. W. Breiby, M. M. Nielsen, T. I. Sölling, M. Giles, I. McCulloch and H. Sirringhaus, *Chem. Mater.*, 2004, **16**, 4772.
12 Y. D. Park, J. K. Park, J. H. Seo, J. D. Yuen, W. H. Lee, K. Cho and G. C. Bazan, *Adv. Energy Mater.*, 2011, **1**, 63.
13 S. K. Park, T. N. Jackson, J. E. Anthony and D. A. Mourey, *Appl. Phys. Lett.*, 2007, **91**, 063514-1.
14 B. H. Lee, S. H. Park, H. Back and K. Lee, *Adv. Funct. Mater.*, 2011, **21**, 487.
15 W. H. Lee, D. H. Kim, Y. Jang, J. H. Cho, M. Hwang, Y. D. Park, Y. H. Kim, J. I. Han and K. Cho, *Appl. Phys. Lett.*, 2007, **90**, 132106-1.
16 S. Hugger, R. Thomann, T. Heinzel and T. Thurn-Albrecht, *Collid. Polym. Sci.*, 2004, **282**, 932.
17 D. H. Kim, Y. D. Park, Y. Jang, S. Kim and K. Cho, *Macromol. Rapid. Commun.*, 2005, **26**, 834.
18 Y. Fu, C. Lin and F. Y. Tsai, *Org. Electron.*, 2009, **10**, 883.
19 Y. D. Park, J. K. Park, W. H. Lee, B. Kang and K. Cho, *J. Mater. Chem.*, 2012, **22**, 11462.
20 S. Nam, D. S. Chung, J. Jang, S. H. Kim, C. Yang, S. K. Kwon and C. E. Park, *J. Electrochem. Soc.*, 2010, **157**, H90.
21 H. Zhou, Y. Zhang, J. Seifter, S. D. Collins, C. Luo, G. C. Bazan, T. Q. Nguyen and A. J. Heeger, *Adv. Mater.*, 2013, **25**, 1646.
22 H. -Y. Park, H. Yang, S. -K. Choi and S. -Y. Jang, ACS. Appl. Mater. Interfaces, 2012, **4**, 214.
23 T. Yamamoto, D. Komarudin, M. Arai, B. L. Lee, H. Suganuma, N. Asakawa, Y. Inoue, K. Kubota, S. Sasaki and T. Fukuda, *J. Am. Chem.*, 1998, **120**, 2047.
24 G. Horowitz, *Adv. Mater.*, 1998, **10**, 365.
25 A. Patil, A. Heeger and F. Wudl, *Chem. Rev. (Washington, D.C.)*, 1988, **88**, 183.
26 P. G. Schroeder, C. B. France, J. B. Park and B. A. Parkinson, *J. Phys. Chem. B*, 2003, **107**, 2253.
27 H. Sandberg, G. Frey, M. Shkunov, H. Sirringhaus and R. Friend, Langmuir, 2002, **18**, 10176.
28 A. Zen, M. Saphiannikova, D. Neher, U. Asawapirom and U. Scherf, *Chem. Mater.*, 2005, **17**, 781.
29 S. Samitsu, T. Shimomura, S. Heike, T. Hashizume and K. Ito, *Macromolecules*, 2008, **41**, 8000.
30 S Nam, J. Jang, H. Cha, T. K. An, S. Park and C. E. Park, *J. Mater. Chem.*, 2012, **22**, 5543.
31 O. Inganäs, W. R. Salaneck, J. -E. Österholm and J. Laakso, *Synth. Met.*, 1988, **22**, 395.
32 Y. D. Park, S. G. Lee, H. S. Lee, D. Kwak, D. H. Lee and K. Cho, *J. Mater. Chem.*, 2011, **21**, 2338.
33 H. Sirringhaus, P. J. Brown, R. H. Friend, M. M. Nielsen, L. Bechgaard, B. M. W. Langeveld-Voss, A. J. H. Spierirg, R. A. J. Janssen, E. W. Meijer and P. Herwig, *Nature*, 1999, **401**, 685.
34 Y. D. Park, J. H. Cho, D. H. Kim, Y. Jang, H. S. Lee, K. Ihm, T. H. Kang, K. Cho, *Electrochem. Solid-State Lett.*, 2006, **9**, G317.
35 M. L. Chabinyc, M. F. Toney, R. S. Kline, I. McCulloch and M. Heeney, *J. Am. Chem. Soc.*, 2007, **129**, 3226.
36 Y. D. Park, H. S. Lee, Y. J. Choi, D. Kwak, J. H. Cho, S. Lee and K. Cho, *Adv. Funct. Mater.*, 2009, **19**, 1200.
37 D. Khim, K.-J. Baeg, J. Kim, M. Kang, S.-H. Lee, Z. Chen, A. Facchetti, D.-Y. Kim and Y.-Y. Noh, *ACS. Appl. Mater. Interfaces*, 2013, **5**, 10745.